Contents lists available at ScienceDirect

Digital Chinese Medicine

journal homepage: http://www.keaipublishing.com/dcmed

Integrating proteomics and targeted metabolomics to reveal the material basis of liver-gallbladder damp-heat syndrome in chronic hepatitis B

LI Ni'ao[a], GONG Yuefeng[b], WANG Jia[a], CHEN Qingqing[a], SU Shibing[a], ZHANG Hua[c*], LU Yiyu[a*]

a. Institute of Interdisciplinary Integrative Medicine Research, Shanghai University of Traditional Chinese Medicine, Shanghai 201203, China

b. Hepatobiliary and Urological Surgery, Qidong Hospital of Traditional Chinese Medicine, Qidong, Jiangsu 226200, China

c. Key Laboratory of Liver and Kidney Diseases (Ministry of Education), Institute of Liver Diseases, Shuguang Hospital Affiliated to Shanghai University of Traditional Chinese Medicine, Shanghai 201203, China

ARTICLE INFO

Article history
Received 21 August 2024
Accepted 13 November 2024
Available online 25 December 2024

Keywords
Liver-gallbladder damp-heat syndrome (LGDHS)
Chronic hepatitis B (CHB)
Proteomics
Targeted metabolomics
Molecular mechanism
Biomarkers

ABSTRACT

Objective To elucidate the biological basis of liver-gallbladder damp-heat syndrome (LGDHS) within the framework of traditional Chinese medicine (TCM) as a complementary diagnostic and therapeutic approach in chronic hepatitis B (CHB).

Methods CHB patients and healthy volunteers were enrolled from Shuguang Hospital Affiliated to Shanghai University of Traditional Chinese Medicine between August 21, 2018 and December 31, 2020. They were divided into three groups: healthy group, LGDHS group, and latent syndrome (LP) group. Proteomic analysis using isobaric tags for relative and absolute quantitation (iTRAQ) was performed to identify differentially expressed proteins (DEPs). Metabolomic profiling via ultra-performance liquid chromatography-tandem mass spectrometry (UPLC-MS/MS) was applied to serum samples to detect differentially regulated metabolites (DMs). Kyoto Encyclopedia of Genes and Genomes (KEGG) and Gene Ontology (GO) enrichment were employed to explore dysregulated pathways. Principal component analysis (PCA) and orthogonal partial least squares discriminant analysis (OPLS-DA) were utilized to visualize group separation and identify key metabolites and proteins contributing to LGDHS differentiation. Receiver operating characteristic (ROC) curve analysis evaluated the diagnostic performance of key biomarkers, while logistic regression models assessed their predictive accuracy. *P* values were corrected for multiple tests using the Benjamini-Hochberg method to control the false discovery rate (FDR). Validation of potential biomarkers was conducted using independent microarray data and real-time quantitative polymerase chain reaction (RT-qPCR).

Results A total of 150 participants were enrolled, including healthy group (n = 45), LGDHS group (n = 60), and LP group (n = 45). 254 DEPs from proteomics data and 72 DMs from metabolomic profiling were identified by PCA and OPLS-DA. DEPs were mainly enriched in immune and complement pathways, while DMs involved in amino acid and energy metabolism. The integrated analysis identified seven key biomarkers: α1-acid glycoprotein (*ORM1*), asparagine synthetase (*ASNS*), solute carrier family 27 member 5 (*SLC27A5*), glucosidase II alpha subunit (*GANAB*), hexokinase 2 (*HK2*), 5-methyltetrahydrofolate-homocysteine methyltransferase (*MTR*), and maltase-glucoamylase (*MGAM*). Microarray validation confirmed the diagnostic potential of these genes, with area under the curve (AUC) values for

*Corresponding author: LU Yiyu, E-mail: yiyulu@shutcm.edu.cn. ZHANG Hua, E-mail: lnutcmzh@126.com.

Peer review under the responsibility of Hunan University of Chinese Medicine.

DOI: 10.1016/j.dcmed.2025.01.005

Citation: LI NA, GONG YF, WANG J, et al. Integrating proteomics and targeted metabolomics to reveal the material basis of liver-gallbladder damp-heat syndrome in chronic hepatitis B. Digital Chinese Medicine, 2024, 7(4): 320-331.

ROC analysis ranging from 0.536 to 0.759. Among these, *ORM1*, *ASNS*, and *SLC27A5* showed significant differential ability in differentiating LGDHS patients (P = 0.016, P = 0.035, and P < 0.001, respectively), with corresponding AUC of 0.749, 0.743, and 0.759, respectively. A logistic regression model incorporating these three genes demonstrated an AUC of 0.939, indicating a high discriminatory power for LGDHS. RT-qPCR further validated the differential expression of *ORM1* and *SLC27A5* between LGDHS and LP groups (P = 0.011 and P = 0.034, respectively), with *ASNS* showing a consistent trend in expression (P = 0.928).

Conclusion This study integrates multi-omics approaches to uncover the molecular mechanisms underlying LGDHS in CHB. The identification of biomarkers *ORM1*, *ASNS*, and *SLC27A5* offers a solid basis for the objective diagnosis of LGDHS, contributing to the standardization and modernization of TCM diagnostic practices.

1 Introduction

Nowadays, approximately 250 million people worldwide are living with chronic hepatitis B (CHB) infection, particularly in Asia and Sub-Saharan Africa [1]. In China, the prevalence of CHB remains high, with approximately 6% of adults being CHB virus carriers, primarily concentrated in the 35 to 60 years old age group [2]. CHB leads to severe complications such as liver cirrhosis, hepatocellular carcinoma, and liver failure [3]. Despite advancements in antiviral therapies, managing CHB often requires comprehensive strategies to address not only the viral infection but also the resultant liver pathologies and overall health of the patient [4–6]. Therefore, integrating alternative and complementary approaches, such as traditional Chinese medicine (TCM), is crucial to improve therapeutic outcomes.

TCM has emerged as an adjunct in the treatment of chronic liver diseases, including CHB [7–9]. In TCM, diseases are diagnosed based on a combination of symptoms and signs, known as syndromes, and individualized treatments are prescribed accordingly. CHB in TCM is categorized as "hypochondriac pain" "jaundice" and "abdominal distention" reflecting the complex interaction between external pathogenic factors and internal imbalances. Common TCM syndromes associated with CHB include liver Qi stagnation, spleen deficiency with dampness, blood stasis, and liver-gallbladder damp-heat (LGDH). Among these syndromes, LGDH syndrome (LGDHS) is frequently observed in CHB patients [10, 11]. It is characterized by symptoms such as jaundice, hypochondriac pain, nausea, and bitter taste, reflecting the complex pathological changes due to chronic infection and inflammation.

However, the integration of TCM into modern medical practice faces significant challenges, primarily due to the lack of standardized biological evaluation criteria for TCM syndromes [12]. Syndrome differentiation relies heavily on the practitioners' experience, making it difficult to achieve consistent and reproducible diagnoses. This has led to a growing interest in exploring the molecular underpinnings of TCM syndromes to bridge the gap between traditional diagnostic methods and contemporary biomedical standards.

Recent advances in omics technologies provide promising tools to investigate the biological underpinnings of TCM syndromes [13]. Metabolomics, which refers to the comprehensive analysis of small molecules (or metabolites), within cells and tissues, offers insights into metabolic alterations in organisms. These metabolites can reveal important information about how biological systems react to diseases, such as CHB [14]. Besides, proteomics focuses on the large-scale study of proteins, and helps uncover their roles in many biological processes and disease mechanisms [15]. Integrating these two approaches enables researchers to gain a deeper understanding of the molecular mechanisms underlying TCM syndromes and may identify potential biomarkers for their diagnosis and treatment.

The application of proteomics and metabolomics to study TCM syndromes, particularly in CHB patients, represents a novel and interdisciplinary approach [16]. It allows for the investigation of complex biochemical networks and pathways that may be perturbed in the context of LGDHS. For instance, alterations in lipid metabolism [17], amino acid metabolism [18], and inflammatory pathways [19] have been implicated in both CHB and TCM syndrome. In our earlier research, we demonstrated that the cytokine profiles in LGDHS and liver-kidney Yin deficiency (LKYD) syndromes were distinct, reflecting different patterns of immune and inflammatory reactions [20]. Additionally, microarray analyses of microRNA and mRNA revealed significant biological differentiation and identified potential dynamic biomarkers for LGDHS in CHB [10, 21]. By characterizing these changes at the molecular level, researchers can develop a more objective and quantifiable framework for TCM syndrome differentiation. Moreover, exploring the biological basis of TCM syndromes in polygenic complex diseases like CHB requires a robust and comprehensive research design. Multi-center clinical studies employing the systems biology approach are essential to capture the heterogeneity of patient populations and the multifactorial nature of the disease [22, 23].

The integration of proteomics and metabolomics into this study of LGDH syndrome in CHB patients represents a significant advancement in TCM research. By bridging traditional diagnostic methods with modern biological technologies, this approach holds the potential to enhance the understanding, diagnosis, and treatment of TCM syndromes [24]. This study aims to identify key biomarkers and dysregulated metabolic pathways associated with LGDHS in CHB. By integrating proteomics and metabolomics, we seek to uncover the molecular mechanisms underlying LGDHS and establish a more objective and standardized approach for its diagnosis and treatment.

2 Materials and methods

2.1 Participants

In this study, participants were enrolled from Shuguang Hospital Affiliated to Shanghai University of Traditional Chinese Medicine between August 21, 2018 and December 31, 2020. They were divided into three groups: healthy group, LGDHS group, and latent syndrome (LP) group. The study was approved by the Ethics Committee of Shanghai University of Traditional Chinese Medicine (2017-557-40-01), with clinical registration number ChiCTR1800017884. All participants provided written informed consent. Healthy group had no history of viral infections, liver diseases, or other significant health issues.

2.1.1 Western diagnostic criteria of CHB Screening of CHB patients was conducted according to the Guidelines for the Prevention and Treatment of Chronic Hepatitis B [25]. The diagnosis of CHB is established through a combination of clinical history, laboratory findings, and liver function tests, including the presence of HBsAg positivity (detection of HBsAg in the blood), detection of hepatitis B virus DNA (HBV DNA) in serum, to indicate ongoing viral replication. In liver function tests, elevated serum alanine aminotransferase (ALT) or aspartate aminotransferase (AST) levels (> 40 U/L) are indicative of liver inflammation or injury.

2.1.2 TCM diagnostic criteria of CHB For LGDHS and LP groups, screening was based on the Standards of Traditional Chinese Medicine Syndrome Differentiation for Viral Hepatitis [26]. The TCM diagnosis was conducted using the four diagnostic methods (inspection, auscultation and olfaction, inquiry, and palpation). The tongue and pulse characteristics were assessed during the physical examination, and symptom questionnaires were completed for all participants.

(i) LGDHS diagnostic criteria. The diagnostic criteria for LGDHS are based on a combination of primary and secondary symptoms. The primary symptoms include short and reddish urine; a bitter and sticky taste in the mouth; a yellow and greasy tongue coating (mandatory for the diagnosis). The secondary symptoms encompass constipation or loose stools; a dry mouth with thirst but reluctance to drink; epigastric distention and poor appetite; nausea and vomiting; fatigue and lethargy; either a slippery and rapid pulse or soft and rapid pulse. The typical tongue appearance features include a red or deep red tongue color; a yellow and greasy tongue coating; a swollen tongue with possible teeth marks; a moist tongue surface.

The diagnosis is confirmed if at least one primary symptom and two secondary symptoms are present, or if a typical tongue appearance is observed alongside at least one primary or secondary symptom.

(ii) LP diagnostic criteria. The diagnostic criteria for the LP syndrome are based on previous studies [27, 28]. LP patients do not exhibit any identifiable TCM syndromes, according to TCM's four diagnostic methods, and in some cases, the syndrome may remain indeterminate due to insufficient information. LP patients are typically considered the control group in TCM studies to eliminate the influence of any underlying TCM syndrome [21, 28].

2.1.3 Inclusion and exclusion criteria

(i) Inclusion criteria. Healthy participants are required to have no history of liver disease, including chronic hepatitis A, hepatitis B, hepatitis C, or non-alcoholic fatty liver disease. Additionally, they should not have a history of systemic chronic diseases, such as diabetes, hypertension, or cardiovascular disease. The liver function tests of healthy participants should show normal liver function indicator levels, such as serum ALT, AST, and normal total bilirubin levels. Furthermore, they should have no presence of HBV-related markers such as HBsAg, HBV DNA, or hepatitis B core antibody (anti-HBc), indicating no detectable markers of past or present hepatitis B infection.

CHB patients should be diagnosed with CHB infection and aged between 18 and 65 years. Written informed consent was required for participation in the study.

(ii) Exclusion criteria. Individuals younger than 18 or older than 65 years were excluded. Participants were not eligible if they exhibited other liver conditions (e.g., viral hepatitis, fatty liver, autoimmune liver diseases), chronic severe hepatitis, decompensated cirrhosis from hepatitis B, or severe primary conditions affecting the heart, kidneys, lungs, endocrine system, blood, metabolism, and gastrointestinal tract. Additionally, individuals with mental illnesses, or those who are pregnant or lactating, were excluded.

2.1.4 Clinical information collection All patients were diagnosed on their first visit by three senior TCM specialists in the outpatient setting. The clinical information collection team consisted of more than three chief TCM physicians who performed blind assessments of tongue

and pulse characteristics and syndrome classification. The diagnosis of the syndrome by TCM liver disease experts was conducted through a blind assessment process. Positive items from the four diagnostic methods (inspection, auscultation and olfaction, inquiry, and palpation) were extracted, including tongue and pulse characteristics, and a specialized survey form was created for expert evaluation. This form was then reviewed by three senior TCM liver disease specialists, who determined the syndrome classification. The final syndrome classification was determined to ensure its typicality and accuracy. Additionally, the demographic and clinical data of all participants were gathered using electronic medical record (EMR) system, including factors such as age, gender, medical and family history (including inherited conditions), medication history, and assessments of liver function.

2.2 Isobaric tags for relative and absolute quantitation (iTRAQ), protein identification, and relative quantification of proteins

Protein samples from blood plasma for LGDHS, LP, and healthy groups were collected. An equal amount of 10 different samples were mixed to produce a sample pool for each TCM syndrome group, resulting in three biological replicates per group.

Protein extraction involved the use of 100 μg of protein from blood plasma in each group with radioimmunoprecipitation assay buffer (RIPA) (Beyotime, China), followed by centrifugation at 12 000 g for 20 min at 4 °C. Protein concentration was determined using the bicinchoninic acid (BCA) assay (Beyotime, China). Extracted proteins were digested with trypsin (Promega, USA) overnight at 37 °C. Samples were then labeled with iTRAQ reagents (AB SCIEX, USA) and fractionated by strong cation exchange (SCX) chromatography on an Agilent 1200 high-performance liquid chromatography (HPLC) system, following the manufacturer's instructions. The labeled peptides were mixed and analyzed by liquid chromatography coupled with tandem mass spectrometry (LC-MS/MS). Protein identification and quantification were performed using MaxQuant 1.3.0.5. The LC-MS/MS data were searched against the UniProt human database. A ratio of protein expression between the two groups (< 0.8 or > 1.25) was considered significant.

2.3 Metabolomics analysis

2.3.1 Serum sample preparation Whole blood was collected in vacutainer tubes and serum was separated by precipitation at 4 °C for 2 h, followed by centrifugation at 3 000 × g for 15 min. The serum was then aliquoted and stored at – 80 °C to maintain stability and prevent repeated freeze-thaw cycles.

Standards for targeted metabolites were obtained from Sigma-Aldrich (USA), Stellaroids (USA), and TRC (Canada). Each standard was precisely weighed and dissolved in appropriate solvents, including water, methanol, sodium hydroxide solution, or hydrochloric acid solution, to create individual standard stock solutions with a concentration of 5.0 mg/mL. These individual solutions were combined to form a mixed standard stock solution for testing purposes [29, 30].

Serum samples were thawed gradually in a salt ice bath to minimize metabolite degradation. Aliquots of 25 μL serum were placed into precooled 96-well plates, which were processed on the Biomek 4000 workstation (Biomek 4000, Beckman Coulter Inc.). To each well, 100 μL of precooled methanol and internal standard solution were added, and the samples were centrifuged at 3 000 × g for 30 min (Allegra X-15R, Beckman Coulter Inc.). The supernatants (30 μL) were then transferred to a new 96-well plate, and 20 μL of freshly prepared derivatization reagent was added. The plates were sealed and incubated at 30 °C for 60 min for derivatization. Each sample was subsequently diluted with 350 μL of ice-cold 50% methanol solution, incubated at – 20 °C for 20 min, and centrifuged at 4 000 g for 30 min at 4 °C. The supernatants (135 μL) were transferred to another 96-well plate, and 15 μL of internal standard solution was added. The derivatized standard stock solution was then added in a gradient to the left wells, and the plate was sealed for LC-MS/MS analysis. All prepared samples were analyzed within 48 h of extraction and derivatization.

2.3.2 Ultra-performance liquid chromatography-tandem mass spectrometry (UPLC-MS/MS) conditions and detection Chromatographic separation was performed using an ACQUITY UPLC system equipped with a BEH C18 1.7 μm VanGuard pre-column (2.1 mm × 5 mm) and a BEH C18 1.7 μm analytical column (2.1 mm × 100 mm). The column was kept at 40 °C and the sample chamber at 10 °C. The mobile phase consisted of 0.1% formic acid in water (solvent A) and a mixture of 90% acetonitrile and 10% isopropyl alcohol (solvent B). The elution gradient was programmed as follows: 0 – 1 min (5% B), 1 – 12 min (5% – 80% B), 12 – 15 min (80% – 95% B), 15 – 16 min (95% – 100% B), 16 – 18 min (100% B), 18 – 18.1 min (100% – 5% B), and 18.1 – 20 min (5% B). The flow rate was set to 0.4 mL/min, and 5 μL of sample was injected. The mass spectrometry conditions were optimized with an ion source temperature of 150 °C, 1.5 kV for positive ion mode (ESI+), 2.0 kV for negative ion mode (ESI–), a desolvation temperature of 550 °C, and a desolvation gas flow rate of 1 000 L/h.

Raw data from UPLC-MS/MS were converted to NetCDF format using QuanMET (V2.0) and imported into a customized MATLAB (V7.0) script for processing. The data were normalized using an internal standard, centralized, and homogenized using Pareto scaling in SIMCA-P (V14.0) before further analysis.

2.4 Microarrays data from independent cohort for validation

Venous blood from participants was drawn, treated with 150 μL ethylenediaminetetraacetic acid (EDTA), and stored at – 20 °C. Total RNA was isolated following a previously described two-step protocol. Leukocyte RNA was extracted from whole blood using TRIzol® reagent (Invitrogen, USA), and quality was assessed with a NanoDrop (Thermo Scientific, ND-1 000). Biotin-labeled cDNAs were hybridized to the NimbleGen *Homo sapiens* 12x135K Array (Roche, A6484-00-01), which evaluated over 135 000 transcripts, including 4 049 well-characterized human genes. Microarray preprocessing was conducted using GenePix software. Raw expression values underwent $\log_2$ transformation and quantile normalization. Probes with a signal-to-noise ratio (SNR) below 2 were deemed unreliably expressed.

2.5 Blood sample collection and RNA extraction

Peripheral blood mononuclear cells (PBMCs) were separated from blood samples using Ficoll density gradient centrifugation and stored at – 80 °C. Total RNA was extracted from these cells using a previously established two-step protocol. Leukocytes isolated from whole blood were processed for total RNA extraction with TRIzol® reagent (Invitrogen, USA) and subsequently stored at – 80 °C. The quality of the extracted RNA was assessed using the NanoDrop spectrophotometer (Thermo Scientific, ND-1000).

2.6 Real-time quantitative polymerase chain reaction (RT-qPCR)

Before initiating RT-qPCR, reverse transcriptase was added for the amplification and detection of RNA targets. Gene expression was verified using RT-qPCR. Blood samples were collected, and RNA was extracted according to the method detailed in our previous study. RNA samples with an A260/A280 ratio between 1.8 and 2.1 were deemed suitable for further processing. 1 μg of total RNA was converted to cDNA in a 20 μL reaction volume.

The primers used for the RT-qPCR assay are listed in Table 1. Each RT-qPCR assay mixture had a total volume of 25 μL, containing 2 μL of SYBR Green qPCR Master Mix, 0.4 μmol/L primers, and 0.5 μL of template cDNA. The cycling conditions were 95 °C for 5 min, followed by 40 cycles of 95 °C for 30 s, 54 °C for 15 s, and 72 °C for 15 s, with a final step at 83 °C for 1 s. The comparative Ct (ΔCt) value method was used for quantitative analysis relative to β-actin expression. Gene expression levels were compared using Student's t test, with statistical significance set at $P < 0.05$.

2.7 Bioinformatic analysis

The significance of Kyoto Encyclopedia of Genes and Genomes (KEGG) and Gene Ontology (GO) enrichment analyses was assessed using the hypergeometric test with the clusterProfiler package in R (V 4.4.1). Functions with $P < 0.05$ were considered significantly enriched. Network visualization was carried out using Cytoscape (V3.8.2). The list of compound labels was uploaded to MetaboAnalyst (V6.0), where the Pathway Analysis module was used to perform pathway enrichment analyses and identify the most relevant pathways related to the study conditions. For multivariate analysis, the data matrix was processed with SIMCA-P (V14.0). Unsupervised principal component analysis (PCA) was utilized to describe and identify differences and relationships between samples. To identify different metabolites, an orthogonal partial least squares discriminant analysis (OPLS-DA) model was constructed.

2.8 Statistical analysis

For nonparametric comparisons, the Mann-Whitney U test was applied. The Chi-square test was used to evaluate the independence between categorical variables, such as gender distribution across different groups. Receiver operating characteristic (ROC) curve analysis was conducted to evaluate the diagnostic performance of identified biomarkers. Logistic regression models were used to assess the relationship between biomarkers and clinical outcomes. Differential expression analysis of metabolites and proteins was performed, with adjustments made for multiple testing corrections using the Benjamini-Hochberg method to control the false discovery rate (FDR). All visualizations, including box plots and ROC curves, were generated using GraphPad Prism (V9.4.1). $P < 0.05$ was considered statistically significant.

Table 1 Validated genes and their primer sequences by RT-qPCR

Gene symbol	Forward primer	Reverse primer
Solute carrier family 27 member 5 (*SLC27A5*)	AGAGGACCGGACACATACA	GTAGACTTCCCAGATCCGAATAG
Asparagine synthetase (*ASNS*)	TTACAACAGTTCGTGCTTCAGTAGG	TCCAGAGAAGATCACCACGCTATC
Orosomucoid 1 (*ORM1*)	CATTCCCAAGTCAGATGTCGTGTAC	TCTCCTTCTCGTGCTGCTTCTC
β-Actin (*ACTB*)	ACAGAGCCTCGCCTTTGCCG	ACATGCCGGAGCCGTTGTCG

3 Results

3.1 Clinical information for TCM syndrome identification

In this study, a total of 150 participants were enrolled, including 45 healthy volunteers and 105 CHB patients. These patients include healthy group (n = 45), LP group (n = 45), and LGDHS group (n = 60). The demographic characteristics showed no significant differences in age, gender, and body mass index (BMI) between the groups (P > 0.05). Liver function indexes did not show a significant difference between CHB patients with LP and LGDHS (P > 0.05). Compared with healthy group, the CHB patients including LP and LGDHS groups showed significantly different levels of ALT, AST, direct bilirubin (DBIL), γ-glutamyl transpeptidase (γ-GT), total protein (TP), total bile acid (TBA), and alkaline phosphatase (ALP) (P < 0.05) (Table 2). No significant difference was observed in total bilirubin (TBIL) and indirect bilirubin (IBIL) in the disease groups compared with healthy group (P > 0.05). The HBV DNA indexes did not differ significantly between CHB patients with LP and LGDHS (P > 0.05) (Table 2).

3.2 iTRAQ data revealing dysregulated proteins in CHB patients with LGDHS

To obtain a comprehensive proteomic landscape of LGDHS and identify potential biomarkers, the PBMCs from participants were subjected to iTRAQ-based proteomic analyses, including patients with LGDHS group (n = 12), LP group (n = 12), and healthy group (n = 12). A total of 840 proteins were identified. The PCA showed that the proteomic data could separate the three groups clearly (Figure 1A), revealing an altered proteomic landscape of LGDHS. Differential expression analysis identified a total of 254 differential expression proteins (DEPs) that were significantly separated (P < 0.05, Figure 1B). KEGG pathway enrichment of DEPs showed that the most enriched pathway was complement and coagulation cascades (Figure 1C). GO analysis showed the DEPs were most enriched in immune-related terms including immune effector process and acute inflammatory response (Figure 1D).

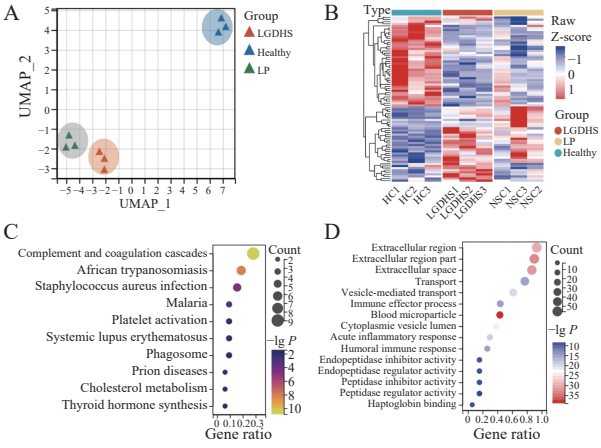

Figure 1 iTRAQ-based proteomic analyses of CHB patients with LGDHS from the discovery cohort
A, the PCA of healthy, LP, and LGDHS groups based on the proteomic data. B, the heatmap of the 62 DEPs between healthy, LP, and LGDHS groups. C, the top 10 KEGG pathways enriched by DEPs. D, the top 15 GO terms enriched by DEPs.

3.3 UPLC-MS/MS detecting dysregulated metabolism compound of CHB patients with LGDHS

To explore the metabolic basis of LGDHS in CHB, we used 90 samples for metabolomics analysis, including LGDHS group (n = 30), LP group (n = 30), and healthy group (n = 30). Seventy-two deregulated metabolites (DMs) were identified. As shown in Figures 2A – 2C, there was a clear difference in the liver metabolic profile among LGDHS, LP, and healthy groups in OPLS-DA score plots and PCA in a three-dimensional (3D) view, suggesting that LGDHS is significantly different from LP in metabolomic profiling (Figure 2D). The metabolic pathways significantly altered in LGDHS group mainly included alanine, aspartate, and glutamate metabolism, arginine biosynthesis, glyoxylate and dicarboxylate metabolism,

Table 2 Comparison of clinical characteristics among the three groups (mean ± SD)

Group	Age (year)	Gender (male/famale)	BMI	HBV DNA (lg)	ALT (U/L)	AST (U/L)	TBIL (μmol/L)
Healthy (n = 45)	35.80 ± 4.91	27/18	22.07 ± 2.36	—	17.79 ± 10.18	20.79 ± 4.65	14.42 ± 4.18
LP (n = 45)	32.23 ± 6.05	24/21	22.09 ± 2.20	6.89 ± 1.34	64.25 ± 37.01*	48.58 ± 31.54*	14.84 ± 4.94
LGDHS (n = 60)	35.50 ± 9.44	32/28	22.49 ± 2.65	3.92 ± 2.72	70.17 ± 74.04*	50.76 ± 34.36*	16.72 ± 6.29

Group	IBIL (μmol/L)	DBIL (μmol/L)	ALB (g/L)	γ-GT (U/L)	TP (mmol/L)	TBA (μmol/L)	ALP (U/L)
Healthy (n = 45)	11.41 ± 3.42	3.02 ± 0.85	41.86 ± 5.74	20.69 ± 11.51	69.50 ± 9.97	2.78 ± 1.74	73.07 ± 14.37
LP (n = 45)	10.62 ± 4.25	4.23 ± 0.85*	43.29 ± 1.80*	35.17 ± 16.82*	75.56 ± 4.36*	6.35 ± 3.58*	80.83 ± 26.32*
LGDHS (n = 60)	11.43 ± 4.40	5.29 ± 2.57*	44.80 ± 4.08*	38.59 ± 22.75*	75.74 ± 7.62*	13.13 ± 23.17*	93.93 ± 33.61*

*P < 0.05, compared with healthy group.

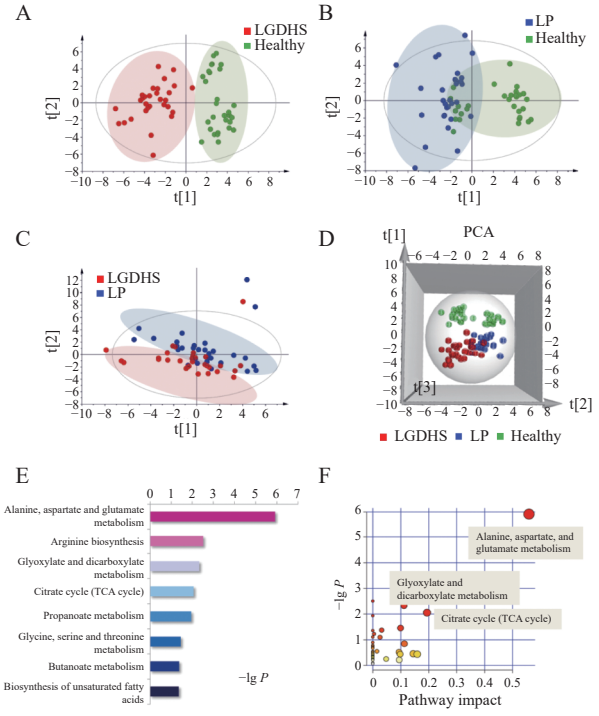

Figure 2 Metabolomic profiling of blood by UPLC-MS/MS

A, OPLS-DA plot for healthy and LGDHS groups. B, OPLS-DA plot for LP and healthy groups. C, OPLS-DA plot for LP and LGDHS groups. D, 3D PCA of healthy, LP, and LGDHS groups. E, KEGG of significantly DMs ($P < 0.05$ and fold change > 2) between LGDHS and LP groups. F, metabolic pathway impact prediction based on the KEGG online database. The – lg P values from the pathway enrichment analysis are indicated on the horizontal axis, and the impact values are indicated on the vertical axis.

citrate cycle, propanoate metabolism, glycine, serine, and threonine metabolism, butanoate metabolism, and biosynthesis of unsaturated fatty acids (Figure 2E and 2F).

3.4 Integrated proteomic and metabolomic joint analyses

The protein-metabolite interaction network was generated for DEPs, the DMs, and the functional pathways enriched by DMs or DEPs. This provides a comprehensive visualization of the interactions between functionally related metabolites and proteins identified from iTRAQ and UPLC-MS/MS. The protein–metabolite interaction consists of 52 nodes connected via 71 edges (Figure 3). The KEGG pathways can be categorized by energy metabolism-related pathways (histidine metabolism, alanine, aspartate, and glutamate metabolism, arginine biosynthesis, aminoacyl-tRNA biosynthesis, lysine degradation, and glyoxylate and dicarboxylate metabolism), amino acid metabolism-related pathways [β-alanine metabolism, propanoate metabolism, D-glutamine and D-glutamate metabolism, and citrate cycle (TCA cycle)], and disease-related pathways (complement and coagulation cascades, GABAergic synapse, African trypanosomiasis, and HIF-1 signaling pathway).

Figure 3 The interaction network of protein, metabolite, and pathway constructed by DMs and DEPs

3.5 Construction of DMs-related genes network and candidate marker moleculars for LGDHS

Metabolism-related molecules are important in TCM syndrome formation. We first used MetaboAnalyst in Cytoscape 3.8 to locate the DMs-related enzyme genes. Sixty-two DMs are related to 148 metabolic enzyme-encoding genes and DMs related genes network was also constructed (Figure 4A). KEGG enrichment analysis showed that these genes were most enriched in pathways such as amino acids, alanine, aspartate, glutamate metabolism, and carbon metabolism (Figure 4B). The enriched GO term showed similar results (Figure 4C). We organized two cohorts of genes, named test cohort (the DEPs and DMs-related enzyme genes) and known

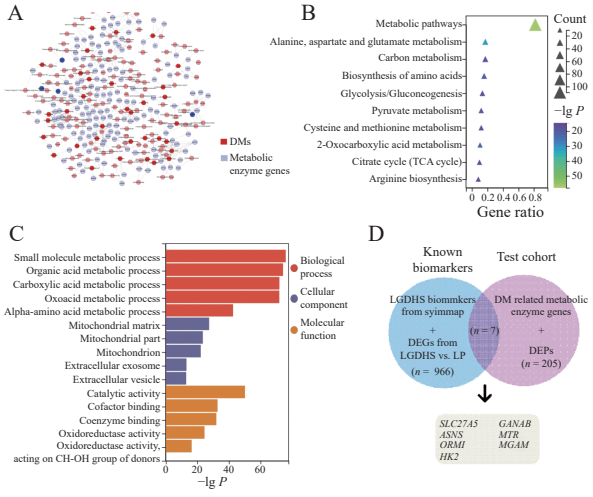

Figure 4 Metabolite-to-gene interaction and identification of candidate marker moleculars for LGDHS

A, network linking DMs and metabolic enzyme genes. B, the top 15 KEGG pathways enriched by DMs-related metabolic genes. C, GO terms enriched by DMs-related metabolic genes. D, Venn analysis between these known biomarkers cohort and test cohort to screen the potential LGDHS markers.

biomarkers cohort [gene biomarkers of LGDHS from the SymMap database and the 223 potential transcriptional differential expressed genes (DEGs) biomarkers from our previous study [11] (DEGs from LGDHS vs. LP)] (Figure 4D). The interactions between these two cohorts of molecules were seen as the potential LGDHS marker from this study. The interactions results showed that seven genes were uncovered, they are solute carrier family 27 member 5 (*SLC27A5*), asparagine synthetase (*ASNS*), glucosidase II α subunit (*GANAB*), hexokinase 2 (*HK2*), 5-methyltetrahydrofolate-homocysteine methyltransferase (*MTR*), maltase-glucoamylase (*MGAM*), and α1-acid glycoprotein (*ORM1*) (Figure 4D).

3.6 Validation in independent microarray data of CHB patients

To validate whether these genes were potential molecular markers of LGDHS syndrome in CHB, we applied an independent cohort of LGDHS group (n = 30), LP group (n = 30), and healthy group (n = 16) to measure the expression levels of these genes using microarray. We also used ROC analyses to estimate the diagnosis abilities of these genes. We conducted ROC analyses to evaluate the diagnostic potential of several genes. These results suggest that *SLC27A5*, *ASNS*, and *ORM1* showed significantly different expression patterns among LGDHS, LP, and healthy groups. *SLC27A5* showed a strong performance with an AUC of 0.759 (P = 0.007, 95% CI: 0.607 4 – 0.910 8), followed closely by *ASNS* (AUC = 0.743, P = 0.013, 95% CI: 0.566 7 – 0.920 2) and *ORM1* (AUC = 0.749, P = 0.007, 95% CI: 0.576 9 – 0.921 1). *MTR* demonstrated moderate diagnostic ability (AUC = 0.694, P = 0.034, 95% CI: 0.526 1 – 0.861 4). In contrast, *HK2* (AUC = 0.567, P = 0.464, 95% CI: 0.378 3 – 0.755 7) and *GANAB* (AUC = 0.591, P = 0.328, 95% CI: 0.411 1 – 0.770 7) showed no significance in ROC analysis. *MGAM* also lacked statistical significance (P = 0.536, 95% CI: 0.354 2 – 0.717 6) (Figure 5).

According to the previous functional enrichment data and ROC analysis, we choose the *SLC27A5*, *ASNS*, and *ORM1* as our potential biomarkers of LGDHS. Furthermore, we applied a step-wise logistic regression model to combine the three genes to distinguish between LGDHS and LP. The logistic model (P = LGDHS) = – 28.631 + 4.707 × *SLC27A5* + 2.883 × *ASNS* – 1.42 × *ORM1* was used to construct the ROC curve. The diagnostic performance of the logistic panel was also evaluated by ROC analysis. The AUC for the panel was 0.939 (P < 0.001; 95% CI; 0.845 0 – 1.000) (Figure 5H). This suggested that these three key genes had the potential to be diagnostic markers for LGDHS.

3.7 Validation in independent CHB patients using RT-qPCR

The expression levels of *ORM1*, *ASNS*, and *SLC27A5* was further validated in an independent group of CHB patients and healthy participants using RT-qPCR. The study included 60 participants, comprising LGDHS (n = 30), LP (n = 15), and healthy (n = 15) groups. The mRNA expression levels of *ORM1*, *ASNS*, and *SLC27A5* were significantly differentially expressed between the LGDHS and healthy groups (P = 0.027, P = 0.003, and P = 0.011, respectively). Transcripts of *ORM1* in LGDHS group were significantly increased when compared with LP group (P = 0.011) (Figure 6A). Transcripts of *SLC27A5* in LGDHS group were significantly decreased compared with LP group (P = 0.034) (Figure 6B). Although the expression level of *ASNS* in LGDHS group was not significantly downregulated between LGDHS and LP groups (P > 0.05), the expression trend was consistent with the microarray expression data (Figure 6C).

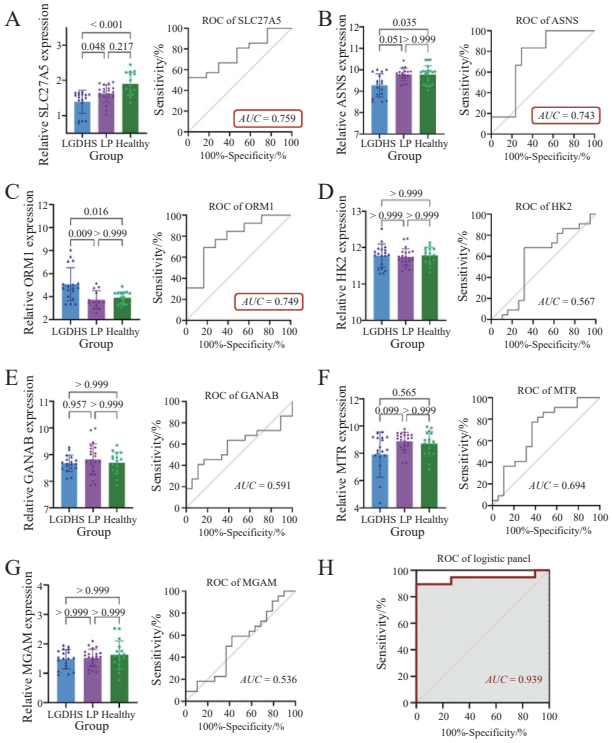

Figure 5 Relative mRNA expression levels and ROC curves in the diagnosis of LGDHS and LP groups

A, *SLC27A5*. B, *ASNS*. C, *ORM1*. D, *HK2*. E, *GANAB*. F, *MTR*. G, *MGAM*. H, ROC of logistic panel.

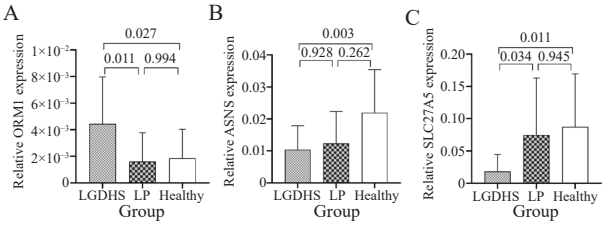

Figure 6 Gene expression levels of *ORM1*, *ASNS*, and *SLC27A5* measured by RT-qPCR

A, *ORM1*. B, *ASNS*. C, *SLC27A5*.

4 Discussion

The systems biology approach has advanced our understanding of the biological underpinnings of TCM syndromes within the domain of substance basis. This study aims to elucidate the scientific nature of TCM syndromes and contribute to their standardization based on data. Through the collection and proteomic analysis of clinical samples, we found no significant differences in general laboratory indicators between CHB patients with LGDHS and those with LP. However, protein expression analysis in LGDHS group revealed significant differences in gene expression compared with LP group and healthy group, as evidenced by PCA, which could clearly distinguish among the three groups, underscoring the biological distinctiveness of LGDHS.

4.1 Metabolic pathways in LGDHS

Our study, aligning with previous findings, indicates that syndromes are closely related to metabolomics, each exhibiting distinct metabolomic profiles. This guided us to conduct targeted metabolomic detection in the three groups. LGDHS was found to be associated with disturbances in metabolic pathways such as amino acid metabolism involving the transformation and degradation of amino acids and glucose metabolism disorders [31], consistent with the results of this study. Gut microbiota and metabolome alterations in differentiating syndromes like Shi-re (damp-heat) and Ping-he (harmonious constitution) [32]. Specifically, LU et al. [21] noted significant changes in alanine, aspartate, and glutamate metabolism as liver damage in LGDHS patients worsened. Our multi-omics joint analysis further corroborates the intricate involvement of LGDHS in energy metabolism, complement-related pathways, and amino acid metabolism, providing a comprehensive understanding of its metabolic reprogramming.

4.2 Identification and validation of biomarkers

Through the integration of DMs and DEPs, along with transcriptomic data and the SymMap database, we identified key enzyme genes relevant to LGDHS. Independent microarray validation and RT-qPCR experiments confirmed significant differential expression of *ORM1*, *ASNS*, and *SLC27A5* between LGDHS and LP groups, consistent with microarray findings.

Elevated levels of *ORM1* have been associated with various inflammatory conditions and liver diseases [33]. The involvement of *ORM1* has been reported in modulating immune responses and maintaining endothelial barrier function, particularly crucial during inflammatory states [34]. Increased serum levels of *ORM1* have been observed in patients with chronic liver diseases, such as cirrhosis and hepatocellular carcinoma, indicating its role as a biomarker for liver pathology [35]. Moreover, *ORM1* has been implicated in drug binding and transport, impacting the pharmacokinetics of various medications in patients with liver disease [36]. The upregulation of *ORM1* in LGDHS patients is in line with the observed hepatic inflammation and immune response activation.

ASNS, an enzyme involved in the synthesis of asparagine from aspartate, is pivotal in the adaptive response to amino acid starvation, activating pathways that support cell growth and survival [37]. In the context of liver disease, upregulation of *ASNS* has been observed in hepatocellular carcinoma and liver fibrosis, where it contributes to the metabolic adaptations required for tumor growth and survival under nutrient-limited conditions [38, 39]. Additionally, *ASNS* expression is regulated by the amino acid response pathway and is essential for maintaining cellular homeostasis during metabolic stress [40]. The increased expression of *ASNS* indicates a shift towards metabolic adaptations necessary for cell survival under the stress conditions associated with LGDHS.

SLC27A5 encodes a protein involved in fatty acid transport and metabolism [41]. It plays a pivotal role in hepatic lipid homeostasis and is crucial for maintaining energy balance within liver cells. Dysregulation of *SLC27A5* expression has been associated with metabolic disorders and liver diseases, including steatosis and hepatitis [42, 43]. Study has also shown that *SLC27A5* is involved in bile acid conjugation and metabolism, linking it to the hepatic handling of bile acids and their role in liver disease [42]. Furthermore, genetic variations in *SLC27A5* have been associated with altered lipid profiles and increased risk of liver disease in various populations [44]. The differential expression of *SLC27A5* underscores its involvement in the altered lipid metabolism seen in LGDHS, further substantiating its role in the disease's metabolic reprogramming.

4.3 Significance and limitations of the study

This study provides significant contributions to understanding the molecular basis of TCM syndromes, particularly in the context of LGDHS in CHB patients. By integrating multi-omics methods, we identified three potential biomarkers that are strongly associated with LGDHS. These biomarkers not only possess diagnostic potential but also offer insights into the metabolic and inflammatory pathways underlying LGDHS, encompassing amino acid metabolism, lipid transport, and immune regulation.

However, the study's integration of proteomics and metabolomics, while providing valuable insights into the molecular basis of LGDHS in CHB, is constrained by the relatively small sample size, which limits the broader applicability of these findings. Additionally, the study's patient cohort was region-specific, which may not fully

represent LGDHS characteristics in more diverse populations. Utilizing professional software, such as G*Power, to calculate and justify sample sizes in future studies, in addition to incorporating regionally and clinically diverse patient cohorts, would substantially enhance the robustness and generalizability of our findings. Furthermore, including additional controls, such as non-CHB individuals with LGDHS symptoms, would strengthen the study's conclusions. Although we identified three biomarkers (*ORM1*, *ASNS*, and *SLC27A5*), further validation in larger and independent cohorts is essential to solidify their diagnostic relevance. Validation through functional assays to confirm the biomarkers' roles in the biological mechanisms of LGDHS, will be pursued in future studies to enhance the robustness of our conclusions.

5 Conclusion

This study underscores the interconnection between LGDHS and pathways influencing immunity and complement systems, as well as the metabolomic alterations in amino acids and energy metabolism. We also identified potential marker genes, such as *ORM1*, *ASNS*, and *SLC27A5* for differentiating LGDHS. These findings not only contribute to the further understanding of the biological basis of TCM syndromes but also pave the way for the development of precise diagnostic and therapeutic approaches in the management of CHB.

Fundings

National Natural Science Foundation of China (82274183), Shanghai Municipal Health Commission's special clinical research project in the health industry (202240243), and Science and Technology Innovation Program of Science and Technology Commission of Shanghai Municipality (STCSM) (20ZR1453700).

Competing interests

The authors declare no conflict of interest.

References

[1] PONDÉ RAA, AMORIM GSP. Elimination of the hepatitis B virus: a goal, a challenge. Medicinal Research Reviews, 2024, 44(5): 2015–2034.

[2] LIU ZQ, LIN CQ, MAO XH, et al. Changing prevalence of chronic hepatitis B virus infection in China between 1973 and 2021: a systematic literature review and meta-analysis of 3 740 studies and 231 million people. Gut, 2023, 72(12): 2354–2363.

[3] SONGTANIN B, CHAISRIMANEEPAN N, MENDÓZA R, et al. Burden, outcome, and comorbidities of extrahepatic manifestations in hepatitis B virus infections. Viruses, 2024, 16(4): 618.

[4] MA H, YAN QZ, MA JR, et al. Overview of the immunological mechanisms in hepatitis B virus reactivation: implications for disease progression and management strategies. World Journal of Gastroenterology, 2024, 30(10): 1295–1312.

[5] SINGH KP, AVIHINGSANON A, ZERBATO JM, et al. Predictors of liver disease progression in people living with HIV-HBV co-infection on antiretroviral therapy. eBioMedicine, 2024, 102: 105054.

[6] ZHANG SS, CHAU HT, TUN HM, et al. Virological response to nucleos(t)ide analogues treatment in chronic hepatitis B patients is associated with Bacteroides-dominant gut microbiome. eBioMedicine, 2024, 103: 105101.

[7] ZHOU R, YANG LP, ZHANG BB, et al. Clinical impact of hepatic steatosis on chronic hepatitis B patients in Asia: a systematic review and meta-analysis. Journal of Viral Hepatitis, 2023, 30(10): 793–802.

[8] XIA Y, LI X, MAN RY, et al. Clinical efficacy and safety of TCM prescriptions combined with nucleoside (acid) analogues in treating chronic hepatitis B: a meta-analysis. Digital Chinese Medicine, 2021, 4(3): 170–179.

[9] CAO X, ZHANG NY, CHEN HN, et al. Exploring the mechanism of JiGuCao capsule formula on treating hepatitis B virus infection via network pharmacology analysis and *in vivo*/*vitro* experiment verification. Frontiers in Pharmacology, 2023, 14: 1159094.

[10] LU YY, FANG ZY, ZENG T, et al. Chronic hepatitis B: dynamic change in traditional Chinese medicine syndrome by dynamic network biomarkers. Chinese Medicine, 2019, 14: 52.

[11] PAN YQ, GUO JC, HU N, et al. Distinct common signatures of gut microbiota associated with damp-heat syndrome in patients with different chronic liver diseases. Frontiers in Pharmacology, 2022, 13: 1027628.

[12] LIU YD, XU J, YU ZC, et al. Ontology characterization, enrichment analysis, and similarity calculation-based evaluation of disease-syndrome-formula associations by applying SoFDA. iMeta, 2023, 2(2): e80.

[13] LI J, ZHU N, WANG YQ, et al. Application of metabolomics and traditional Chinese medicine for type 2 diabetes mellitus treatment. Diabetes, Metabolic Syndrome and Obesity: Targets and Therapy, 2023, 16: 4269–4282.

[14] FAN HN, ZHAO ZM, HUANG K, et al. Serum metabolomics characteristics and fatty-acid-related mechanism of cirrhosis with histological response in chronic hepatitis B. Frontiers in Pharmacology, 2023, 14: 1329266.

[15] JIA XC, HE XY, HUANG CT, et al. Protein translation: biological processes and therapeutic strategies for human diseases. Signal Transduction and Targeted Therapy, 2024, 9(1): 44.

[16] YE XY, HE XZ, HU ZT, et al. Metabolomic analysis identifies dysregulation of lipid metabolism in the immune clearance phase of chronic hepatitis B patients. Journal of Pharmaceutical and Biomedical Analysis, 2024, 239: 115900.

[17] CANG S, LIU R, JIN W, et al. Integrated DIA proteomics and lipidomics analysis on non-small cell lung cancer patients with TCM syndromes. Chinese Medicine, 2021, 16(1): 126.

[18] ZHU Y, GENG SY, ZHU FY. The efficacy of Chaihu-Guizhi-Ganjiang Decoction on chronic non-atrophic gastritis with gallbladder heat and spleen cold syndrome and its metabolomic analysis: an observational controlled before-after clinical trial[letter. Drug Design, Development and Therapy, 2024, 18: 4527–4528.

[19] LU YY, LI MY, ZHOU QM, et al. Dynamic network biomarker analysis and system pharmacology methods to explore the therapeutic effects and targets of Xiaoyaosan against liver

cirrhosis. Journal of Ethnopharmacology, 2022, 294: 115324.
[20] LU YY, ZHAO Y, SONG YN, et al. Serum cytokine profiling analysis for Zheng differentiation in chronic hepatitis B. Chinese Medicine, 2015, 10: 24.
[21] LU YY, ZHAO CQ, WANG CB, et al. The effect and mechanism of Qingre Huashi formula in the treatment of chronic hepatitis B with Gan-Dan-Shi-Re syndrome: an integrated transcriptomic and targeted metabolomic analysis. Journal of Ethnopharmacology, 2024, 319: 117092.
[22] ZHANG YK, YAO R, LI L, et al. Medication rule and mechanism of traditional Chinese medicine in treating metabolism-associated fatty liver disease based on bioinformatics technology. Digital Chinese Medicine, 2023, 6(3): 257–271.
[23] LIU L, WANG H. The recent applications and developments of bioinformatics and omics technologies in traditional Chinese medicine. Current Bioinformatics, 2019, 14(3): 200–210.
[24] LI X, LIU ZQ, LIAO J, et al. Network pharmacology approaches for research of traditional Chinese medicines. Chinese Journal of Natural Medicines, 2023, 21(5): 323–332.
[25] WANG GQ, WANG FS, ZHUANG H, et al. Guidelines for the Prevention and Treatment of Chronic Hepatitis B (2019 version). Journal of Clinical Hepatology, 2019, 35(12): 2648–2669.
[26] LI XH, YANG HS, LI FY, et al. The Standards of Traditional Chinese Medicine Syndrome Differentiation for Viral Hepatitis. Journal of Clinical Hepatology, 2017, 33(10): 1839–1846.
[27] YANG MD, CHEN XL, XIE XZ, et al. TCM syndromes distribution of liver cancer and colorectal cancer with "different diseases with same syndrome" and its association with clinical laboratory Indicators. Modernization of Traditional Chinese Medicine and Materia Medica-World Science and Technology, 2019, 21(11): 2461–2468.
[28] ZHAO CQ, HONG C, CHEN L, et al. Study of material base on Hepatitis B Cirrhosis of Gan Dan Shi Re Pattern and Gan Shen Yin Xu Pattern. Modernization of Traditional Chinese Medicine and Materia Medica-World Science and Technology, 2020, 22(4): 1121–1131.
[29] XIE GX, WANG L, CHEN TL, et al. A metabolite array technology for precision medicine. Analytical Chemistry, 2021, 93(14): 5709–5717.
[30] NI Y, ZHAO LJ, YU HY, et al. Circulating unsaturated fatty acids delineate the metabolic status of obese individuals. eBioMedicine, 2015, 2(10): 1513–1522.
[31] WEI WQ, JI SP. Cellular senescence: molecular mechanisms and pathogenicity. Journal of Cellular Physiology, 2018, 233(12): 9121–9135.
[32] CHEN JY, CHENG JR, LI F, et al. Gut microbiome and metabolome alterations in traditional Chinese medicine damp-heat constitution following treatment with a Chinese patent medicine and lifestyle intervention. Phytomedicine, 2024, 131: 155787.
[33] YUE L, XU XZ, DAI SP, et al. Orosomucoid 1 promotes colorectal cancer progression and liver metastasis by affecting PI3K/AKT pathway and inducing macrophage M2 polarization. Scientific Reports, 2023, 13(1): 14092.
[34] YIN DM, YUAN D, SUN RJ, et al. Identification of ORM1, vWF, SPARC, and PPBP as immune-related proteins involved in immune thrombocytopenia by quantitative LC-MS/MS. Clinical Proteomics, 2023, 20(1): 24.
[35] QIN XY, HARA M, ARNER E, et al. Transcriptome analysis uncovers a growth-promoting activity of orosomucoid-1 on hepatocytes. eBioMedicine, 2017, 24: 257–266.
[36] COSTA AP, COURT MH, VILLARINO NF, et al. Canine orosomucoid (alpha-1 acid glycoprotein) variants and their influence on drug plasma protein binding. Journal of Veterinary Pharmacology and Therapeutics, 2021, 44(1): 116–125.
[37] STAKLINSKI SJ, CHANG MC, YU F, et al. Cellular and molecular characterization of two novel asparagine synthetase gene mutations linked to asparagine synthetase deficiency. Journal of Biological Chemistry, 2022, 298(9): 102385.
[38] YAN JY, FANG XW, FENG YY, et al. Identification of key genes associated with the progression of liver fibrosis to hepatocellular carcinoma based on iTRAQ proteomics and GEO database. Annals of Hepatology, 2022, 27(3): 100681.
[39] ZHOU Q, LI LJ, SHA FF, et al. PTTG1 reprograms asparagine metabolism to promote hepatocellular carcinoma progression. Cancer Research, 2023, 83(14): 2372–2386.
[40] THOMAS TM, MIYAGUCHI K, EDWARDS LA, et al. Elevated asparagine biosynthesis drives brain tumor stem cell metabolic plasticity and resistance to oxidative stress. Molecular Cancer Research, 2021, 19(8): 1375–1388.
[41] NIE D, TANG X, DENG HJ, et al. Metabolic enzyme SLC27A5 regulates PIP4K2A pre-mRNA splicing as a noncanonical mechanism to suppress hepatocellular carcinoma metastasis. Advanced Science, 2024, 11(5): e2305374.
[42] WU K, LIU Y, XIA J, et al. Loss of SLC27A5 activates hepatic stellate cells and promotes liver fibrosis via unconjugated cholic acid. Advanced Science, 2024, 11(2): e2304408.
[43] XU FL, WU XH, CHEN C, et al. SLC27A5 promotes sorafenib-induced ferroptosis in hepatocellular carcinoma by downregulating glutathione reductase. Cell Death & Disease, 2023, 14(1): 22.
[44] WANG JY, QIAO YY, SUN HR, et al. Decreased SLC27A5 suppresses lipid synthesis and tyrosine metabolism to activate the cell cycle in hepatocellular carcinoma. Biomedicines, 2022, 10(2): 234.

联合蛋白质组学和靶向代谢组学揭示慢性乙型肝炎中肝胆湿热证的物质基础

李妮奥[a], 龚跃峰[b], 王佳[a], 陈清清[a], 苏式兵[a], 张华[c*], 陆奕宇[a*]

a. 上海中医药大学交叉科学研究院, 上海 201203, 中国
b. 启东市中医院肝胆泌尿外科, 江苏 启东 226200, 中国
c. 上海中医药大学附属曙光医院肝病研究所肝肾疾病教育部重点实验室, 上海 201203, 中国

【摘要】目的 阐明肝胆湿热证（LGDHS）在中医框架内作为慢性乙型肝炎（CHB）辅助诊疗手段的生物学基础。**方法** 本研究于 2018 年 8 月 21 日至 2020 年 12 月 31 日期间从上海中医药大学附属曙光医院招募 CHB 患者和健康志愿者，并将他们分为三组：健康组、LGDHS 组和潜在症状（LP）组。使用基于同位素标记相对和绝对定量（iTRAQ）的蛋白质组学分析，以识别差异表达蛋白（DEPs）。通过超高效液相色谱串联质谱（UPLC-MS/MS）对血清样本进行代谢组学分析，鉴定差异代谢物（DMs）。采用京都基因与基因组百科全书（KEGG）和基因本体论（GO）富集分析，探讨 LGDHS 失调的生物通路。使用主成分分析（PCA）和正交偏最小二乘判别分析（OPLS-DA）进行组间分离和关键代谢物及蛋白的筛选。通过受试者工作特征（ROC）曲线分析评估关键生物标志物的诊断性能，使用逻辑回归模型评估其预测准确性。多重检验采用 Benjamini-Hochberg 方法对多重测试进行 *P* 值校正以控制伪发现率（FDR）。此外，利用独立的微阵列数据和实时定量聚合酶链反应（RT-qPCR）验证潜在生物标志物。**结果** 研究共招募了 150 名参与者，包括健康组（$n = 45$）、LGDHS 组（$n = 60$）和 LP 组（$n = 45$）。通过 PCA 和 OPLS-DA 从蛋白质组学中共鉴定 254 个 DEPs，代谢组学分析中发现 72 个 DMs。DEPs 主要富集于免疫和补体通路，DMs 涉及氨基酸和能量代谢通路。综合分析筛选出 7 个关键生物标志物，包括类粘蛋白 1（*ORM1*）、天冬酰胺合成酶（*ASNS*）、溶质载体家族 27 成员 5（*SLC27A5*）、葡萄糖苷酶 IIα 亚基（*GANAB*）、己糖激酶 2（*HK2*）、5-甲基四氢叶酸-同型半胱氨酸甲基转移酶（*MTR*）和麦芽糖酶-葡糖淀粉酶（*MGAM*）。微阵列验证显示这些基因在 ROC 曲线分析中的曲线下面积（AUC）值范围为 0.536 至 0.759。其中，*ORM1*、*ASNS* 和 *SLC27*A5 在区分 LGDHS 患者方面表现出显著的差异能力（分别为 $P = 0.016$、$P = 0.035$、$P < 0.001$），对应的 AUC 值分别为 0.749、0.743、0.759。逻辑回归模型结合这三个基因后，AUC 达到 0.939，显示出较高的鉴别能力。RT-qPCR 进一步验证了 *ORM1* 和 *SLC27A5* 在 LGDHS 与 LP 组之间的差异表达（分别为 $P = 0.011$、$P = 0.034$），*ASNS* 也显示出和基因芯片一致的表达趋势（$P = 0.928$）。**结论** 本研究通过整合多组学技术，阐明了 CHB 中 LGDHS 的分子机制。生物标志物 *ORM1*、*ASNS* 和 *SLC27A5* 的鉴定为 LGDHS 的客观诊断奠定了基础，有助于推动中医证候诊断的标准化和现代化。

【关键词】肝胆湿热证；慢性乙型肝炎；蛋白质组学；靶向代谢组学；分子机制；生物标志物